



## Review

# A review of functionalized carbon nanotubes and graphene for heavy metal adsorption from water: Preparation, application, and mechanism



Jiang Xu <sup>a,b</sup>, Zhen Cao <sup>a</sup>, Yilin Zhang <sup>b</sup>, Zilin Yuan <sup>b</sup>, Zimo Lou <sup>c</sup>, Xinhua Xu <sup>c,\*</sup>,  
Xiangke Wang <sup>d</sup>

<sup>a</sup> State Key Laboratory of Estuarine and Coastal Research, East China Normal University, Shanghai, 200062, China

<sup>b</sup> Department of Civil and Environmental Engineering, Carnegie Mellon University, Pittsburgh, 15213, USA

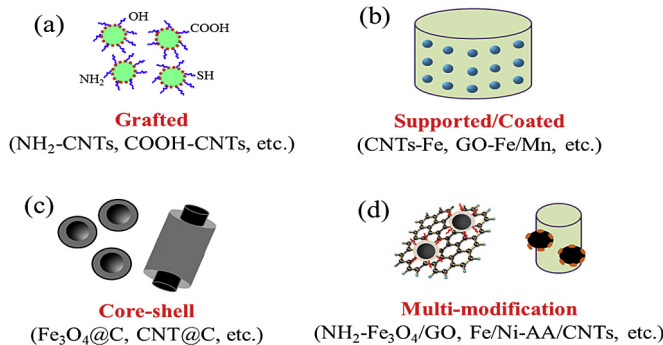
<sup>c</sup> Department of Environmental Engineering, Zhejiang University, Hangzhou, Zhejiang 310058, China

<sup>d</sup> School of Environment and Chemical Engineering, North China Electric Power University, Beijing, 102206, China

## HIGHLIGHTS

- Removal of heavy metals from water has drawn wide attention.
- Various functionalized carbon nanotube and graphene nanomaterials were stated.
- Effects of water environmental chemistry on heavy metals removal were discussed.
- Adsorption isotherms, kinetics, thermodynamics, and pathways were discussed.
- Some research prospects were proposed for future studies and application.

## GRAPHICAL ABSTRACT



## ARTICLE INFO

## Article history:

Available online 19 December 2017

Handling Editor: Chang-Ping Yu

## Keywords:

Heavy metals  
Functionalized  
Carbon nanotube  
Graphene  
Adsorption

## ABSTRACT

Carbon-based nanomaterials, especially carbon nanotubes and graphene, have drawn wide attention in recent years as novel materials for environmental applications. Notably, the functionalized derivatives of carbon nanotubes and graphene with high surface area and adsorption sites are proposed to remove heavy metals via adsorption, addressing the pressing pollution of heavy metal. This critical review assesses the recent development of various functionalized carbon nanotubes and graphene that are used to remove heavy metals from contaminated water, including the preparation and characterization methods of functionalized carbon nanotubes and graphene, their applications for heavy metal adsorption, effects of water chemistry on the adsorption capacity, and decontamination mechanism. Future research directions have also been proposed with the goal of further improving their adsorption performance, the feasibility of industrial applications, and better simulating adsorption mechanisms.

© 2017 Elsevier Ltd. All rights reserved.

\* Corresponding author.

E-mail address: [\(X. Xu\).](mailto:xuxinhua@zju.edu.cn)

**List of acronyms**

AA	Activated alumina	nZVI	Nanoscale zero-valent iron
LDH	Layered double hydroxide	DES	Deep eutectic solvents
AC	Activated carbon	OMC	Ordered mesoporous carbon
M-CHAP	magnetic carbonate hydroxyapatite	DFT	Density functional theory
BET	Brunauer-Emmett-Teller	PAA	Polyacrylic acid
MC-N	magnetic carbon-iron reduced by Fe(NO <sub>3</sub> ) <sub>3</sub>	EDA	Ethylenediamine
CB[6]	Cucurbit[6]uril	PANI	Polyaniline
MC-O	magnetic carbon-iron reduced by Fe <sub>3</sub> O <sub>4</sub>	Fe <sub>2</sub> O <sub>3</sub>	Maghemite
CMK	Nanoporous carbons	RGO	Reduced graphene oxide
MIO	Magnetic iron oxide	GO	Graphene oxide
CMPEI	Carboxymethylated polyethyleneimine	SMG	Smart magnetic graphene
MPTS	Mercaptopropyltriethoxysilane	HA	Humic acid
CNTs	Carbon nanotubes	VP	2-vinylpyridine
MWCNTs	Multi-walled carbon nanotubes	HEG	Hydrogen exfoliated graphene
CS	Chitosan	WHO	World Health Organization
NPs	Nanoparticles	HMO	Hydrous manganese dioxide
DBSA	Dodecyl-benzene-sulfonic-acid	XPS	X-ray photoelectron spectroscopy
		IL	Ionic liquid

**Contents**

1.	Introduction .....	352
2.	Functionalized carbon nanotubes and graphene: preparations and structures .....	353
2.1.	Preparations .....	353
2.2.	Structures .....	353
3.	Applications of functionalized carbon nanotubes and graphene for aqueous heavy metal adsorption .....	355
3.1.	Adsorption of four most concerned heavy metals (Hg, Pb, Cr, and Cd) .....	355
3.2.	Adsorption of aqueous As(III)/(V) and other heavy metals .....	355
4.	Effects of water environmental chemistry on heavy metal removal .....	357
4.1.	Temperature .....	357
4.2.	pH value .....	357
4.3.	Ionic strength and coexisting ions .....	358
5.	Mechanism of heavy metal removal by functionalized carbon nanotubes and graphene nanomaterials .....	358
5.1.	Adsorption isotherms .....	358
5.2.	Adsorption kinetics .....	359
5.3.	Adsorption thermodynamics .....	359
5.4.	Other pathways that accompany adsorption .....	359
6.	Future research prospects .....	359
6.1.	Functional nanomaterials for treating combined pollution .....	359
6.2.	Sustainability of nanomaterials .....	360
6.3.	Computational simulations .....	360
6.4.	Other recommendations for future research .....	360
7.	Conclusions .....	361
	Acknowledgements .....	361
	References .....	361

**1. Introduction**

Water is the most essential and important component for living beings on Earth. In the last century, anthropogenic water demand has increased sevenfold due to the quadrupled global population (Pendergast and Hoek, 2011). Approximately 2.6 billion people have gained access to an improved drinking water source since 1990, while 663 million people still lack improved drinking water sources in 2015, according to the report of “Progress on Sanitation and Drinking Water-2015 Update and MDG Assessment” by the World Health Organization (WHO). The number of people living in water scarce regions will increase to about 3.9 billion by 2030, as

estimated by the World Water Council. As a result of rapid developments in urbanization, industrialization, and agricultural activities, the removal of heavy metals from contaminated waters has become a major environmental concern. Many metals are essential nutrients in trace amounts, but become significant threats to environmental and human health at high concentrations. Heavy metals are non-biodegradable and can accumulate in the environment and living organisms (Hashim et al., 2011; Xu et al., 2017a, b). Neurological, mental, and other various adverse effects are caused by exposure to, transportation of, and accumulation of heavy metals, especially Hg(II), Pb(II), Cr(VI), Cd(II), and As(III)/(V) (Meng et al., 2014; Sima et al., 2015; Dong et al., 2017; Rehman et al.,

**Table 1**

Maximum acceptable level of selected heavy metal ions in drinking water in different countries ( $\mu\text{g L}^{-1}$ ).

Heavy metals	WHO	E.U.	U.S.	Canada	Australia	Japan	China
Hg	6	1	2	1	1	0.5	1
Pb	10	10	15	10	50	50	10
Cr	50	50	100	50	50	50	50
Cd	3	5	5	5	2	10	5
As	10	10	10	25	7	10	10

2017). As shown in Table 1, the maximum allowable concentrations of these five heavy metal ions in drinking water have been strictly set by the WHO and many countries. The availability of freshwater is an important issue for human health and social development (Machell et al., 2015).

Much work has been carried out on the removal of aqueous heavy metals by various methods, including adsorption, filtration, precipitation, reduction, ion exchange, and electrochemical removal (Xu et al., 2013c, 2016c; Xiao et al., 2016; Huang et al., 2017; Sounthararajah et al., 2017; Sun et al., 2017; Xu et al., 2017b). The general advantages and disadvantages of commonly used methods for the removal of aqueous heavy metals are given in Fig. 1. Of these methods, adsorption is more versatile and widely used for the removal of aqueous heavy metals. It has many advantages, such as simple operation, low cost, good pH tolerance, and large industrial processing capacity. In addition, high efficiency and selectivity can also be achieved via purposeful functionalization. A simple and cheap method that does not require a large investment or energy inputs is desirable for wastewater treatment.

Nanomaterials are currently on the cutting edge of material science research and are gradually finding applications in our daily life, including life science, energy, and environmental applications. Carbon nanomaterials, with their high specific surface areas and large pore volumes, have remained at the forefront of nanotechnology. Many forms, especially carbon nanotubes (CNTs) and graphene, have been widely used to remove aqueous Hg(II), Pb(II), Cr(VI), Cd(II), As(III)/(V), Co(II), U(VI), and other metal ions (Mauter and Elimelech, 2008; Zhao et al., 2011a, b; Tian et al., 2012; Liu et al., 2013b; Perreault et al., 2015; Ihsanullah Abbas et al., 2016). Based on the high surface area, scalable production, tunable surface chemistry, non-corrosive property, and presence of surface oxygen-containing functional groups of CNTs and graphene nanomaterials, the adsorption performance are generally better than other conventional adsorbents, such as zero valent iron, iron oxide, zeolite,

silica, titanium dioxide, chitosan, and polymer (George et al., 2016; Huang et al., 2016; Lv et al., 2012; Morillo et al., 2015; Vunain et al., 2016; Yurekli, 2016). However, pure nanomaterials have some limitations, and carbon-based nanocomposites or nanohybrids with more and controlled functionalities are attracting attention for environmental applications (Chang and Wu, 2013; Sun and Xu, 2014). Scientific and technological research face challenges with the durability, functionality, and performance of advanced nanomaterials, which are increasingly important in environmental applications (Chabot et al., 2014).

Over the past decade, nanomaterials with multiple functions have been rapidly developed through academic pursuit based on commercial realities. The concepts of functionalization at the nanoscale level have already led to new aqueous heavy metal treatments with state-of-the-art performance parameters—rapid removal, high capacity, good selectivity, easy separation, and satisfactory reusability. Based on the potential advantages of functionalized CNTs and graphene, we present a brief overview of various functionalized CNTs and graphene that are used to adsorb heavy metals from contaminated water, and mainly focus on their applications and mechanisms for adsorption of heavy metals. Meanwhile, the effects of water environmental chemistry on their adsorption behaviors are also discussed. In Section 6, we propose some interesting research prospects in the field of functionalized nanomaterials.

## 2. Functionalized carbon nanotubes and graphene: preparations and structures

### 2.1. Preparations

Due to the non-corrosive property, tunable surface chemistry, high surface area, and presence of surface oxygen-containing functional groups, carbon nanotubes and graphene materials have been chosen as platforms to build new adsorbents with enhanced or more functions (Perreault et al., 2015). Functionalization of CNTs and graphene for environmental applications are mostly fabricated via chemical methods, including purely chemical processes (i.e., chemical oxidation and deposition) and extended chemical process (i.e., electrochemical, sol-gel, microemulsion, and hydrothermal methods) (Cho et al., 2010; Khin et al., 2012). These methods usually contain a precursor of chemical reductant or photoreductant for nanomaterial generation, and a supportive, stabilizer, or additive agent for obtaining the desired function (Parambath et al., 2011; Ojani et al., 2014). Chemical reactions are more selective and straightforward than other processes, and can integrate functional groups with carbon nanomaterials to obtain multiple functions (Zhao et al., 2011a, b). Some typical methods for functionalization of CNTs and graphene are shown in Table 2. After preparation, characterization is an indispensable procedure to obtain the micromorphology, chemical composition, surface area, surface functional groups, and other properties of the nanomaterials, especially focusing on the difference between raw and functionalized CNTs and graphene. Characterizations provide important support for understanding the mechanisms involved.

### 2.2. Structures

Carbon-based nanomaterials have great potential for use in water treatment, and should be designed to obtain suitable structures and properties. Therefore, the deliberate design of the structures and properties of nanomaterials is usually performed with the intention of obtaining synergistic multi-functionalities or solving a specific problem. The properties of nanomaterials are not only size dependent, but also structure dependent. Supported,

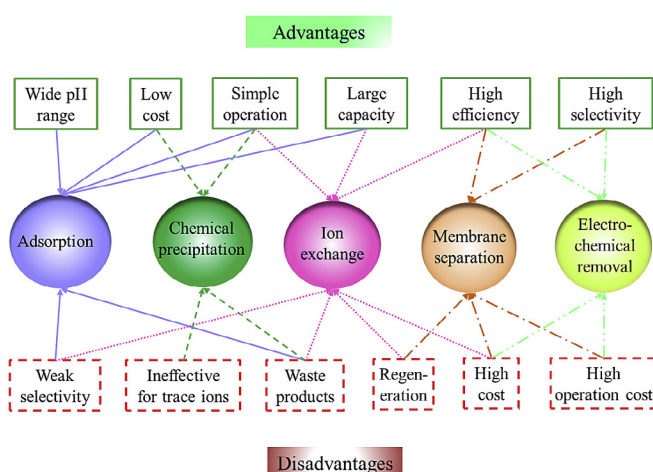


Fig. 1. Common methods for the removal of aqueous heavy metals.

**Table 2**

Chemical synthesis methods for various functionalized nanomaterials.

Nanomaterial	Method	Ref.
Oxidized MWCNTs	Simple chemical reaction: MWCNTs $\xrightarrow[\text{sonicated,3h,40}^{\circ}\text{C}]{\text{H}_2\text{SO}_4:\text{HNO}_3(3:1)}$ filtered dried oxidized MWCNTs	(Vuković et al., 2010)
NH <sub>2</sub> -MWCNTs	Simple chemical reaction: oxidized MWCNTs $\xrightarrow[\text{sonicated 4h,40}^{\circ}\text{C}]{\text{EDA,N-HATU}}$ filtered dried NH <sub>2</sub> – MWCNTs	(Vuković et al., 2011)
CNTs-FeS	Chemical vapor deposition: ethanol+ferrocene+thiophene $\xrightarrow[\text{argon flow,pyrolysis}]{\text{oxidation1h}}$ CNTs – Fe <sub>2</sub> O <sub>3</sub> $\xrightarrow[\text{air flow,400}^{\circ}\text{C}]{\text{reduction1h}}$ sulfur powder $\xrightarrow[\text{argon flow,600}^{\circ}\text{C}]{\text{filtered}}$ CNTs – FeS	(Ma et al., 2015)
Bare GO	Hummers method: Graphite powder $\xrightarrow[\text{vibrant agitation}]{\text{NaNO}_3,\text{H}_2\text{SO}_4,66^{\circ}\text{C}}$ KMnO <sub>4</sub> , <20°C $\xrightarrow[\text{35}\pm 3^{\circ}\text{C},30\text{min}]{\text{diluted}}$ $\xrightarrow[\text{vibrant agitation 98}^{\circ}\text{C},15\text{min}]{3\% \text{ H}_2\text{O}_2\text{ treating}}$ GO vibrant agitation, filtered,washed,dispersed	(Hummers and Offeman, 1958)
Sulfur-RGO	Green one-step method: GO $\xrightarrow[\text{Citrus limon juice,acidic}]{\text{Na}_2\text{S}_2\text{O}_3,\text{sonicated,1h}}$ disproportionation,30min S – RGO	(Thakur et al., 2013)
PB-GO	Modified Hummers method: Graphite powder $\xrightarrow[\text{hotplate,80}^{\circ}\text{C}]{\text{K}_2\text{S}_2\text{O}_8,\text{P}_2\text{O}_5,\text{H}_2\text{SO}_4}$ diluted with DI water filtered,washed $\xrightarrow[\text{dried,overnight}]{\text{H}_2\text{SO}_4,0^{\circ}\text{C};\text{KMnO}_4}$ stirring,icebath, <20°C $\xrightarrow[\text{35}^{\circ}\text{C}]{\text{stirred2h}}$ diluted,stirred2h $\xrightarrow[30\% \text{ H}_2\text{O}_2\text{ treating}]{\text{ice bath, }<50^{\circ}\text{C}}$ GO ice bath, <50°C filtered,washed,dispersed	(Xu et al., 2008)

coated, grafted, core-shell, and multiple modification types are common structures of functionalized CNTs and graphene nanomaterials for aqueous heavy metal removal.

The surfaces of carbon nanomaterials always contain some functional groups, which play an important role in the adsorption process. Thus, many studies have been performed to further increase the abundance of pre-existing functional groups (such as COOH and OH) or graft other functional groups (such as NH<sub>2</sub> and SH) onto the surface of carbon nanomaterials as a way to enhance their adsorptive capacities (Vuković et al., 2010; El-Sheikh et al., 2011; Hadavifar et al., 2014). Additional performance can be obtained by coating the carbon nanomaterials with other nanoparticles (NPs); The carbon-supported nanomaterials are generally porous and stable, with large specific surface area and good adsorptive capacities (Lv et al., 2011; Xu et al., 2012b; Tang et al., 2016).

The core-shell is a novel structure in materials chemistry, and has been attracting increasing attention due to its many applications in biomedicine, catalysis, electronics, pharmaceuticals, and environmental pollution control. Core-shell carbon-based nanomaterials usually consist of an inner material (core) and an outer material (shell). Different combinations of materials have been produced and tested, such as Fe<sub>3</sub>O<sub>4</sub>@C, RGO@Al<sub>2</sub>O<sub>3</sub>, C@Si, and CNT@C (Cui et al., 2009; Hahm et al., 2013; Du et al., 2014; Yao et al., 2015; Jastrzębska et al., 2016). However, most of these carbon-based core-shell nanomaterials are used as high-capacity electrodes, and the applications for aqueous heavy metal removal still needs to be studied.

Additionally, more complex nanocomposites have also been fabricated to remove aqueous heavy metals. CNTs and graphene nanomaterials are extensively modified to have multiple properties, such as redox ability to change the form of a heavy metal, magnetic properties for easy separation and recycling of the nanomaterials, and enhanced adsorptive capacity.

### 3. Applications of functionalized carbon nanotubes and graphene for aqueous heavy metal adsorption

#### 3.1. Adsorption of four most concerned heavy metals (Hg, Pb, Cr, and Cd)

Mercury (Hg), Lead (Pb), Chromium (Cr), and cadmium (Cd) are regarded as four of the most concerned heavy metals, which are non-biodegradable, bioaccumulative, and extreme hazardous. Serious threats to plant, animal, and human health are caused by these heavy metals, even at trace levels concentration (Akhavan et al., 2015; Boeing, 2000; Cutting et al., 2010; Gardarin et al., 2010; Lavoie et al., 2015; Zhu et al., 2012). Table 3 shows various functionalized CNTs and graphene nanomaterials that have been used for the adsorption of aqueous heavy metals.

Generally, the interaction between metal ions and the surface oxygen-containing groups plays an important role in adsorption capacity of heavy metals on CNTs and graphene based nanomaterials. As shown in Table 3, the raw CNTs materials usually require acid or oxidation treatments to increase their surface oxygen-containing functional groups, while no additional acid or oxidation treatments are required for graphene, because the as-prepared graphene material already possesses a large number of oxygen-containing functional groups (Zhao et al., 2011a, b).

Note that the toxicity of Cr(VI) is much higher than that of Cr(III), and reduction processes have been required before adsorption or precipitation. For example, functional magnetic carbon-iron nano-adsorbents were prepared by carbonizing cellulose and reducing Fe(NO<sub>3</sub>)<sub>3</sub> or Fe<sub>3</sub>O<sub>4</sub> NPs (MC-N and MC-O, respectively) (Qiu et al.,

2014). MC-N and MC-O were used to remove Cr(VI) through reduction and precipitation, and the nanomaterials could be easily separated by a permanent magnet following the reaction.

In recent years, many studies have focused on magnetic nanocomposites, which have some excellent advantages, with their low cost, environmentally friendly composition, mesoporous nanostructure with a large surface area for rapid adsorption, and easy magnetic retrieval by an external magnetic field for recycling (Han et al., 2009; Xu et al., 2013b; Wang et al., 2010). Generally, magnetic functionalized nanomaterials are prepared to remove heavy metals and then are retrieved by magnetic separation (Fig. 2a), which is a very effective way to recycle the nanomaterials and avoid environmental risks that could result from their release (Wang et al., 2016). In addition, magnetic carbon materials have also been developed to capture other functionalized nanomaterials that used to remove heavy metals. A typical example is presented in Fig. 2b (Shih et al., 2014). Tween 20 functionalized Au NPs were used to remove aqueous Hg(II) from a high-salt matrix (artificial seawater) by reducing Hg<sup>2+</sup> to Hg<sup>0</sup>. The Hg<sup>0</sup> then deposited onto the surfaces of the Tween 20-Au NPs. After the reaction, magnetic and reduced graphite-Fe<sub>3</sub>O<sub>4</sub> NPs were used to collect the Tween 20-Au NPs, and the mixture was further retrieved by a second magnetic field.

#### 3.2. Adsorption of aqueous As(III)/(V) and other heavy metals

As a metalloid element, arsenic (As) contamination of groundwater is affecting millions of people globally, and can cause serious health problems, such as bladder, lung, and skin cancer (Mishra and Ramaprabhu, 2010). The sources of As, the 12th and 20th element in order of natural abundance in the human body and the Earth's crust, respectively, are both naturally occurring (in rock and mineral erosion, volcanic activity, and forest fires) and anthropogenically produced. As has 4 valence states (-3, 0, +3, and +5). As(III) (arsenite) and As(V) (arsenate) are the predominant species of As in water, and As(III) is much more soluble, mobile, and toxic than As(V) (Shih, 2005). Hence, an oxidation process of As(III) to As(V) is usually required.

With the development of nanotechnology, functional nanomaterials have been widely synthesized for effective As removal (Table 3). Iron oxide NPs have commonly been used to remove aqueous As, with an adsorptive capacity for mixed Fe<sub>3</sub>O<sub>4</sub> and Fe<sub>2</sub>O<sub>3</sub> of 5.99 mg g<sup>-1</sup> (Chowdhury et al., 2010). Because this capacity was a bit low, carbon materials with oxygen-containing groups were then induced to support the iron oxides and improve their adsorptive capacity. The maximum adsorptive capacities of As(III) and As(V) by the CNTs-base iron oxides were 24.05 mg g<sup>-1</sup> and 47.41 mg g<sup>-1</sup>, respectively (Chen et al., 2014a).

Since the oxidation rate of As(III) by Mn(IV) complexes was significantly higher than that by Fe(III) complexes, GO-MnFe<sub>2</sub>O<sub>4</sub> nanohybrids were fabricated. The BET surface areas of GO-MnFe<sub>2</sub>O<sub>4</sub> nanohybrids and bare MnFe<sub>2</sub>O<sub>4</sub> nanohybrids were 196 m<sup>2</sup> g<sup>-1</sup> and 91 m<sup>2</sup> g<sup>-1</sup>, respectively (Kumar et al., 2014). The adsorptive capacities of As(III) and As(V) by GO-MnFe<sub>2</sub>O<sub>4</sub> nanohybrids were greatly improved, to 146 mg g<sup>-1</sup> and 207 mg g<sup>-1</sup>, respectively, which was much higher than GO NPs in the absence of Mn(IV) complexes (Mishra and Ramaprabhu, 2011; Paul et al., 2015; Ray and Shipley, 2015).

In addition to the five heavy metals of concern mentioned above, other heavy metals have also been studied due to their wide industrial use and the threats they pose to humans and ecosystems. Other heavy metals that have been studied for removal by functionalized carbon-based nanomaterials include Cu(II), Zn(II), Ni(II), Co(II), and radioactive U(VI) (Table 3).

**Table 3**

Functionalized carbon-based nanomaterials used for aqueous heavy metals removal.

Nanomaterial	BET ( $\text{m}^2 \text{ g}^{-1}$ )	pH	Capacity ( $\text{mg g}^{-1}$ )		Ref.
			Exp.	Cal.	
<b>Hg(II)</b>					
oxidized MWCNTs	N/A	7.0	N/A	3.8	El-Sheikh et al., 2011
MWCNTs-COOH	N/A	4.3	81.6	127.6	Chen et al., 2014b
MWCNTs-OH	N/A	4.3	89.4	120.1	Chen et al., 2014b
SWCNTs-SH	N/A	5.0	74.2	131.6	Bandaru et al., 2013
MWCNTs-iodide	153.0	6.0	100.0	123.5	Gupta et al., 2014
MWCNTs-S	155.3	6.0	100.0	151.5	Gupta et al., 2014
CNTs-MnO <sub>2</sub>	110.4	6.0	14.3	58.8	Moghaddam and Pakizeh, 2015
KMnO <sub>4</sub> -DES-CNTs	199.4	5.5	187.0	250.5	AlOmar et al., 2017
CS-MWCNTs-COOH	N/A	4.0	183.2	181.8	Shawky et al., 2012
CS-MWCNTs	N/A	4.0	167.5	169.4	Shawky et al., 2012
MWCNTs/Fe <sub>3</sub> O <sub>4</sub> -SH	97.2	6.5	63.7	65.5	Zhang et al., 2012
Tween 20-Au/graphite-Fe <sub>3</sub> O <sub>4</sub>	N/A	N/A	N/A	47.6	Shih et al., 2014
Pb(II)					
MWCNTs	N/A	6.0	N/A	15.9	Ren et al., 2011
Acidified MWCNTs	237.3	5.0	85.0	49.7	Wang et al., 2007a
MWCNTs-VP	N/A	6.0	N/A	37.0	Ren et al., 2011
MWCNTs-TiO <sub>2</sub>	N/A	6.0	4.6	137.0	Zhao et al., 2010
CNTs-MnO <sub>2</sub>	275.0	5.0	N/A	78.7	Wang et al., 2007b
SWCNTs-COOH	400.0	5.0	N/A	94.7	Moradi, 2011
CNTs/Fe <sub>3</sub> O <sub>4</sub> -NH <sub>2</sub>	90.7	5.3	37.6	75.0	Ji et al., 2012
CNTs/Fe <sub>3</sub> O <sub>4</sub> -MPTS	97.2	6.5	42.1	65.4	Zhang et al., 2012
GO	430.0	6.8	328.0	367.0	Madadrag et al., 2012
EDTA-GO	623.0	6.8	479.0	525.0	Madadrag et al., 2012
EDTA-RGO	730.0	6.8	204.0	228.0	Madadrag et al., 2012
GO-MnFe <sub>2</sub> O <sub>4</sub>	196.0	5.0	N/A	673.0	Kumar et al., 2014
RGO-nZVI	N/A	5.0	550.0	585.5	Jabeen et al., 2013
CoFe <sub>2</sub> O <sub>4</sub> -GO	212.7	N/A	81.3	82.3	Ma et al., 2015
M-CHAP/GO	106.0	4.5	244.5	246.1	Cui et al., 2015
HMO@GO	383.9	5.0	553.6	512.6	Wan et al., 2016
<sup>a</sup> SMG	165.0	6.5	N/A	6.0	Gollavelli et al., 2013
Cr(VI)					
IL-oxi-MWCNTs	87.4	3.0	2.6	85.8	Krishna Kumar et al., 2015
CNTs-CeO <sub>2</sub>	N/A	7.0	30.2	31.6	Di et al., 2006
DBSA-PANI/MWCNTs	N/A	2.0	49.5	55.6	Kumar et al., 2013
AC-CNTs	755.8	2.0	9.0	8.6	Atieh, 2011
AA-CNTs	203.0	2.0	142.8	264.5	Sankararamakrishnan et al., 2014
NH <sub>2</sub> -Fe <sub>3</sub> O <sub>4</sub> /GO	43.6	4.5	27.3	32.3	Liu et al., 2013a
MC-N	136.3	1.0	327.5	N/A	Qiu et al., 2014
<sup>a</sup> SMG	165.0	6.5	N/A	4.9	Gollavelli et al., 2013
Cd(II)					
Raw MWCNTs	187.6	8.0	1.29	1.3	Vuković et al., 2010
oxidized MWCNTs	78.5	8.0	22.32	22.4	Vuković et al., 2010
EDA-MWCNTs	101.2	8.0	21.23	21.7	Vuković et al., 2010
Al <sub>2</sub> O <sub>3</sub> MWCNTs	109.8	7.0	0.948	27.2	Liang et al., 2015
SWCNTs	400.0	5.0	N/A	21.2	Moradi, 2011
COOH-SWCNTs	400.0	5.0	N/A	55.4	Moradi, 2011
oxidized CNTs	128.0	5.5	N/A	11.0	Li et al., 2003
AA-CNTs	203.0	7.5	200.0	229.9	Sankararamakrishnan et al., 2014
As(III)					
Iron oxide-MWCNTs	N/A	8.0	1.8	4.0	Tawabini et al., 2011
Fe <sub>3</sub> O <sub>4</sub> -MWCNTs	70.1	N/A	N/A	53.2	Mishra and Ramaprabhu, 2010
Fe-MWCNTs	N/A	7.0	210.0	200.0	Alijani and Shariatinia, 2017
EDA-MWCNT/Fe <sup>2+</sup>	198.5	8.0	0.7	N/A	Veličković et al., 2012
MIO-MWCNTs	209.8	7.0	17.2	20.2	Chen et al., 2014a
GO-MnFe <sub>2</sub> O <sub>4</sub>	196.0	6.5	N/A	146.0	Kumar et al., 2014
Fe <sub>3</sub> O <sub>4</sub> -RGO	148	7.0	N/A	13.1	Chandra et al., 2010
HA-RGO-Fe <sub>3</sub> O <sub>4</sub>	0.9	7.0	7.5	8.7	Paul et al., 2015
HEG-electrodes	442.9	6.1	N/A	138.8	Mishra and Ramaprabhu, 2011
GAC-ZrO <sub>2</sub>	903.0	7.6	N/A	12.2	Sandoval et al., 2011
<sup>b</sup> MWCNTs-ZrO <sub>2</sub>	152.0	6.0	$9.8 \times 10^{-2}$	2.0	Addo Ntim and Mitra, 2012
<sup>b</sup> Fe <sub>3</sub> O <sub>4</sub> -MWCNTs	153.0	4.0	$9.7 \times 10^{-2}$	1.7	Addo Ntim and Mitra, 2011
As(V)					
Fe <sub>3</sub> O <sub>4</sub> -MWCNTs	70.1	N/A	N/A	39.1	Mishra and Ramaprabhu, 2010
MIO-MWCNTs	209.8	7.0	36.3	40.8	Chen et al., 2014a
Fe-MWCNTs	N/A	7.0	220.0	200.0	Alijani and Shariatinia, 2017
GO-MnFe <sub>2</sub> O <sub>4</sub>	196.0	4.0	N/A	207.0	Kumar et al., 2014
GO-Fe(OH) <sub>3</sub>	N/A	4.0	23.8	N/A	Zhang et al., 2010
Fe <sub>3</sub> O <sub>4</sub> -RGO	148	7.0	N/A	5.83	Chandra et al., 2010
HA-RGO-Fe <sub>3</sub> O <sub>4</sub>	0.9	7.0	16.0	61.7	Paul et al., 2015
HEG-electrodes	442.9	6.9	N/A	141.9	Mishra and Ramaprabhu, 2011
Mg-Al LDHs/GO	35.4	5.0	183.1	180.3	Wen et al., 2013
<sup>b</sup> MWCNTs-ZrO <sub>2</sub>	152.0	6.0	0.1	5.0	Addo Ntim and Mitra, 2012

**Table 3** (continued)

Nanomaterial	BET ( $\text{m}^2 \text{ g}^{-1}$ )	pH	Capacity ( $\text{mg g}^{-1}$ )		Ref.
			Exp.	Cal.	
<sup>b</sup> EDA-MWCNT/Fe <sup>2+</sup>	198.5	4.0	1.0	18.1	Veličković et al., 2012
<sup>b</sup> Fe <sub>3</sub> O <sub>4</sub> -MWCNTs	153.0	4.0	0.1	0.2	Addo Ntim and Mitra, 2011
<sup>a</sup> SMG	165.0	6.5	N/A	3.3	Gollavelli et al., 2013
Cu(II)					
Oxidized CNTs	N/A	7.0	50.4	64.9	Tofighy and Mohammadi, 2011
Purified MWCNTs	169.7	5.0	37.5	36.8	Ge et al., 2014
Oxidized MWCNTs	N/A	5.0	29	28.5	Li et al., 2003
Sulfonated MWCNTs	28.7	5.0	59.6	43.2	Ge et al., 2014
OH-MWCNTs	111.4	4.9	7.0	10.1	Rosenzweig et al., 2013
COOH-MWCNTs	135.2	4.9	5.5	8.1	Rosenzweig et al., 2013
SWCNTs	400.0	5.0	N/A	22.9	Moradi, 2011
COOH-SWCNTs	400.0	5.0	N/A	72.3	Moradi, 2011
OH-SWCNTs/RGO	N/A	6.8	N/A	256.0	Dichiara et al., 2015
COOH-SWCNTs/RGO	N/A	6.8	N/A	63.0	Dichiara et al., 2015
MWCNTs/Fe <sub>3</sub> O <sub>4</sub>	138.7	5.5	19.0	38.9	Tang et al., 2012
Zn(II)					
Oxidized CNTs	N/A	7.0	58.0	74.6	Tofighy and Mohammadi, 2011
Purified SWCNTs	423.0	N/A	15.4	41.8	Lu et al., 2006
Oxidized MWCNTs	250.0	6.5	2.0	1.1	Mubarak et al., 2013
Ni(II)					
MWCNTs	197.0	5.4	2.9	3.7	Yang et al., 2009
PAA-MWCNTs	N/A	5.4	N/A	3.9	Yang et al., 2009
Oxidized MWCNTs	102.0	6.5	12.5	17.9	Mobasherpour et al., 2012
Co(II)					
Oxidized CNTs	N/A	7.0	69.6	85.7	Tofighy and Mohammadi, 2011
MWCNTs/iron oxide	N/A	6.4	2.9	10.6	Wang et al., 2011
U(VI)					
CB[6]/GO/Fe <sub>3</sub> O <sub>4</sub>	N/A	5.0	N/A	122.5	Shao et al., 2016
Fe <sub>3</sub> O <sub>4</sub> /GO	N/A	5.5	N/A	69.5	Zong et al., 2013
Amidoximated Fe <sub>3</sub> O <sub>4</sub> /GO	N/A	5.0	76.88	92.4	Zhao et al., 2013
CMPEI/CMK	1350.0	4.0	N/A	151.5	Jung et al., 2008

<sup>a</sup> Trace ions removal of 0.1–5.0 mg L<sup>-1</sup>.<sup>b</sup> Trace ions removal of 100 µg L<sup>-1</sup>.

## 4. Effects of water environmental chemistry on heavy metal removal

### 4.1. Temperature

Temperature is a very common parameter affecting physico-chemical reactions and has significant impacts on the adsorption of heavy metals. The reaction rate increases with increasing temperature for endothermic reactions, and decreases with increasing temperature for exothermic reactions.

Generally, higher temperature will reduce the mass transfer resistance and accelerate diffusion. Pb(II), As(III), and As(V) adsorption by MnFe<sub>2</sub>O<sub>4</sub> and GO-MnFe<sub>2</sub>O<sub>4</sub> NPs were enhanced by increased temperature (Kumar et al., 2014). The calculated  $\Delta G^\circ$  values were all negative and decreased with increased temperature, which also indicates that the adsorption process was

spontaneous and more efficient at higher temperatures (Jin et al., 2015). The increased temperature not only increases the number of available active surface sites on the nanomaterials and reduces the thickness and mass transfer resistance of the boundary layer surrounding the nanomaterials; it also allows the ions to be more readily desolvated for removal from the aqueous phase (Gupta and Rastogi, 2008). However, in a reaction with low activation energy, diffusion is not the rate limiting step, and the temperature effects will be insignificant. In the case of exothermic reactions, negative  $\Delta G^\circ$  values increase with increasing temperature, while negative values of  $\Delta H^\circ$  for Hg(II) adsorption onto MWCNTs-SH indicate that the adsorption was more efficient at lower temperatures (Hadavifar et al., 2014).

### 4.2. pH value

Since the pH of the solution will affect the ionic forms of heavy metal ions and functionalized nanomaterials, pH is an important parameter for aqueous heavy metal removal. For example, K<sub>2</sub>Cr<sub>2</sub>O<sub>7</sub> can be dissolved in different ionic forms at different pH values. H<sub>2</sub>CrO<sub>4</sub> is the dominant species at pH < 1.0, while HCrO<sub>4</sub><sup>-</sup> and CrO<sub>4</sub><sup>2-</sup> are predominant at pH 2.0–6.0, and CrO<sub>4</sub><sup>2-</sup> is dominant at pH > 6.0 (Wang et al., 2015a). Aqueous Pb species usually exist as Pb<sup>2+</sup>, Pb(OH)<sup>+</sup>, Pb(OH)<sub>2</sub><sup>-</sup>, or Pb(OH)<sub>2</sub> at different pH values. Specifically, Pb<sup>2+</sup> is the dominant species when pH < 7.0, while Pb(OH)<sub>2</sub> forms and becomes the major species when pH > 8.0 (Vuković et al., 2011). Most of the Hg(II) species exist as Hg<sup>2+</sup> in strongly acidic conditions, while HgOH<sup>+</sup> and Hg(OH)<sub>2</sub> are the main forms in the pH range of 3.0–8.0, and Hg(OH)<sub>2</sub> precipitate is predominant as pH > 8.0 (Wang et al., 2016). As(V) species usually exists in solution as H<sub>3</sub>AsO<sub>4</sub>, H<sub>2</sub>AsO<sub>4</sub><sup>-</sup>, and HAsO<sub>4</sub><sup>2-</sup>. The HAsO<sub>4</sub><sup>2-</sup>

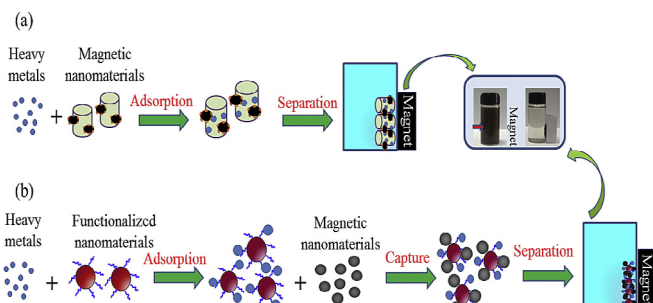


**Fig. 2.** Schematic of the (a) retrieval of magnetic nanomaterials and (b) capture of NPs by magnetic carbon-based nanomaterials.

species is predominant when pH > 7.0, whereas H<sub>2</sub>AsO<sub>4</sub><sup>-</sup> is the major species when pH < 7.0, and H<sub>3</sub>AsO<sub>4</sub> is present at most pH conditions (Lin and Wu, 2001). For As(III), the nonionic H<sub>3</sub>AsO<sub>3</sub> and anionic H<sub>2</sub>AsO<sub>3</sub><sup>-</sup> are the dominant forms when pH < 9.0 and pH > 9.0, respectively (Kwon et al., 2016).

Generally, heavy metals usually exist in the expected forms under acidic condition, and functionalized carbon-based nanomaterials are synthesized according to these expected forms. Therefore, acidic conditions usually favor the removal of heavy metal ions. For example, the removal of Pb(II) by modified MWCNTs was observed to be significantly affected by pH values. When the initial pH values increased from 2.0 to 11.0, the removal efficiency rapidly increased at pH 5.0 and 6.0, slowly decreased in the pH range of 6.0–8.0, and then sharply decreased at pH 8.0–10.0 (Vuković et al., 2011).

In addition to affecting the speciation of heavy metals, the solution pH also affects heavy metal removal with different types of functional groups and nanomaterials. The ionization of the surface acidic groups and charges will also be affected by pH values. For example, the pKa values of carboxylic groups are about 3.0–6.0, which play an important role in the uptake of heavy metal ions. The electrostatic interaction between heavy metal ions and nanomaterials should be considered when making selections for wastewater treatment (Chandra et al., 2010).

#### 4.3. Ionic strength and coexisting ions

The background electrolyte concentration in the solution can be represented by ionic strength. Ionic strength affects the interface potential and thickness of the double layer, especially binding during the adsorption process, which plays an important role in the removal of heavy metal ions by nanomaterials due to their large specific surface areas and strong adsorption abilities. The adsorption type will be affected by the electrolyte concentrations. The background electrolyte ions are in the same plane with the outer-sphere of nanomaterials, which are more susceptible to ionic strength variations than the inner-sphere complexes. For example, the removal rate of Cr(VI) by MWCNTs-supported nZVI was accelerated when the ionic strength was increased from 0 to 0.05 M in our previous study, implying an outer-sphere complexing mechanism and  $\beta$ -plane adsorption (Lv et al., 2011). However, an obvious drop was observed at 0.1 M ionic strength (using NaCl), which might be attributed to the obstruction of Cl<sup>-</sup> on Cr(VI) adsorption by MWCNTs, and the competition of Cl<sup>-</sup> with CrO<sub>4</sub><sup>2-</sup>/HCrO<sub>4</sub> (Pillay et al., 2009).

Coexisting anions and cations are important constituents in the water environment, and the effects on contaminant removal by nanomaterials have been widely reported. Gollavelli et al. investigated the effects of common ions on the Cr(VI) adsorption by smart magnetic graphene (Gollavelli et al., 2013). A decreased trend of Cr(VI) removal was observed with increased SO<sub>4</sub><sup>2-</sup>, probably due to the surface complexation of SO<sub>4</sub><sup>2-</sup> with Fe<sub>2</sub>O<sub>3</sub> and the resulting competition with Cr(VI) species for adsorption sites. Compared to SO<sub>4</sub><sup>2-</sup>, NO<sub>3</sub><sup>-</sup> and Cl<sup>-</sup> had smaller negative charges and did not exhibit obvious effects on the Cr(VI) adsorption. Moreover, coexisting As(V) and Pb(II) ions in the range of 0.1–5.0 mg L<sup>-1</sup> also did not affect Cr(VI) removal by magnetic graphene, and the removal efficiencies of these three coexisting heavy metals were all 99.0%, which indicates that the magnetic graphene is an effective adsorbent for a wide range of heavy metals. In addition, two of the most common cations, Ca(II) and Mg(II), are also usually added to investigate their effects on heavy metal ion removal. (Wan et al., 2016). It was found that Pb(II) adsorption by HMO@GO was not affected by Ca(II) or Mg(II), while a sharp decrease of Pb(II) adsorption by GO was

observed, because the inner-sphere complexation between HMO sites and Pb(II) is specific, while the electrostatic interactions between Pb(II) species and the oxygen-containing groups on GO is nonspecific. Hence, purposeful design of functional nanomaterials would not only enhance the adsorptive capacity of heavy metal ions, but also improve the removal selectivity of foreign ions.

### 5. Mechanism of heavy metal removal by functionalized carbon nanotubes and graphene nanomaterials

#### 5.1. Adsorption isotherms

The adsorptive capacity is the most important indicator and is usually used to evaluate an adsorbent. The theoretical adsorptive capacity is calculated using adsorption isotherm models. The adsorption behavior of heavy metals by functionalized carbon-based nanomaterials are described by isotherm models, such as the Langmuir, Freundlich, Redlich-Peterson, Temkin, and Dubinin-Radushkevich models. These models are expressed using the following equations (Andersson et al., 2011; Xu et al., 2012b; Zhao et al., 2016):

$$\text{Langmuir: } q_e = k_L q_m C_e / (1 + k_L C_e) \quad (1)$$

$$\text{Freundlich: } q_e = k_F C_e^{1/n} \quad (2)$$

$$\text{Redlich - Peterson: } q_e = k_R C_e / (1 + \alpha C_e^\beta) \quad (3)$$

$$\text{Temkin: } q_e = (RT/b_T) \ln(k_T C_e) \quad (4)$$

$$\text{Dubinin - Radushkevich: } q_e = q_m \exp(-k_{DR} \varepsilon^2) \quad (5)$$

where  $q_e$  and  $q_m$  (mg g<sup>-1</sup>) signify the equilibrium and maximum adsorptive capacities, respectively;  $C_e$  (mg L<sup>-1</sup>) is the equilibrium aqueous concentration;  $k_L$  (L mg<sup>-1</sup>) and  $k_F$  (mg g<sup>-1</sup> (mg L<sup>-1</sup>)<sup>n</sup>) represent the adsorptive capacity and the affinity between adsorbate and adsorbent;  $k_R$  (L g<sup>-1</sup>),  $\alpha$  (L g<sup>-1</sup>), and  $\beta$  (dimensionless) are constants;  $k_T$  (L g<sup>-1</sup>) is the equilibrium binding constant;  $b_T$  (J mol<sup>-1</sup>) is related to the heat of adsorption; 1/n (dimensionless) represents the heterogeneity of the adsorbent sites and also indicates the affinity between adsorbate and adsorbent;  $k_{DR}$  (mol<sup>2</sup> kJ<sup>-2</sup>) is related to the mean free energy (kJ mol<sup>-1</sup>) of adsorption and is equal to 1/(2k<sub>DR</sub>)<sup>1/2</sup>, and  $\varepsilon = RT \ln(1 + 1/C_e)$ .

The Langmuir isotherm model is commonly used for monolayer adsorption in which most of the adsorption sites have equal affinities toward the adsorbate, while the Freundlich isotherm model is used to describe a heterogeneous chemisorption process in which the surface is not energetically uniform. The Redlich-Peterson isotherm model is a combination of the Langmuir and Freundlich models, with values  $\beta$  in the range of 0–1. If the value of  $\alpha C_e^\beta$  is much larger than 1, the equation can be approximated by the Freundlich equation, while if  $\beta = 1$ , the equation can be approximated by the Langmuir isotherm model. The Temkin isotherm model is applied to study the heat of adsorption ( $RT/b_T$ ) and the interaction between adsorbates on adsorption isotherms. For example, if the values of  $RT/b_T$  increase with increasing temperature, the adsorption process is endothermic, and the opposite is exothermic (Andersson et al., 2011). The Dubinin-Radushkevich isotherm model is usually used to investigate the type of adsorption process.

Most of the functionalized CNTs and graphene nanomaterials mentioned in this review showed better fit with the Langmuir isotherm model, and the adsorptive capacities of the CNTs and

graphene based nanomaterials for removal of various aqueous heavy metals are in Table 3.

### 5.2. Adsorption kinetics

The adsorption kinetics of aqueous heavy metals by carbon-based nanomaterials are generally well-fitted by the pseudo-first-order, pseudo-second-order, Elovich, and intra-particle diffusion models, which are described in the following equations (Mishra and Ramaprabhu, 2010; Wan et al., 2016).

$$\text{Pseudo first order : } \log(q_e - q_t) = \log q_e - k_1 t / 2.303 \quad (6)$$

$$\text{Pseudo second order : } q_t = k_2 q_e^2 t / (k_2 q_e + 1) \quad (7)$$

$$\text{Elovich kinetics : } q_t = \beta^{-1} \ln(\alpha\beta) + \beta^{-1} \ln t \quad (8)$$

$$\text{Intra - particle diffusion : } q_t = k_i t^{1/2} + C \quad (9)$$

where  $q_t$  and  $q_e$  are the adsorptive capacities ( $\text{mg g}^{-1}$ ) at time  $t$  and at equilibrium, respectively;  $k_1$  ( $\text{min}^{-1}$ ),  $k_2$  ( $\text{min}^{-1}$ ), and  $k_i$  ( $\text{mg g}^{-1} \text{ min}^{-0.5}$ ) are the rate constants of the pseudo-first-order, pseudo-second-order, intra-particle diffusion models, respectively; and  $C$  ( $\text{mg g}^{-1}$ ) is a constant that approximates the thickness of the boundary layer.

Detailed adsorption mechanisms can be inferred from the kinetics model. The pseudo-first-order model of Lagergren has long been widely applied based on the adsorptive capacity. The pseudo-first-order model is based on the assumption that the adsorption rate is controlled by chemical adsorption, which includes the electron transfer and sharing between adsorbate and adsorbent. The Elovich model is an adsorption reaction model that includes chemical reactions. Intra-particle diffusion is usually divided into three steps: (i) diffusion through the liquid film to the adsorbent surface, (ii) diffusion in the pore liquid (intra-particle diffusion), and (iii) adsorption and desorption between the active sites and adsorbate.

### 5.3. Adsorption thermodynamics

The adsorption Gibbs free energy ( $\Delta G^0$ ,  $\text{kJ mol}^{-1}$ ), enthalpy change ( $\Delta H^0$ ,  $\text{kJ mol}^{-1}$ ), and entropy change ( $\Delta S^0$ ,  $\text{kJ mol}^{-1} \text{ K}^{-1}$ ) can be determined by the following equations (Xu et al., 2016b):

$$\Delta G^0 = -RT \ln K_0 \quad (10)$$

$$\Delta G^0 = \Delta H^0 - T\Delta S^0 \quad (11)$$

$$\ln K_0 = \Delta S^0 / R - \Delta H^0 / RT \quad (12)$$

where  $T$  ( $\text{K}$ ) is the system temperature,  $R$  ( $8.314 \text{ J mol}^{-1} \text{ K}^{-1}$ ) is the universal gas constant, and  $K_0$  is the equilibrium constant. The value of  $K_0$  can be obtained from the intercept of  $\ln(q_e/C_e)$  plotted versus  $q_e$ .  $\Delta G^0$  is calculated using Eq. (7).  $\Delta S^0$  and  $\Delta H^0$  are calculated from the intercept and slope of the regression of  $\ln K^0$  versus  $1/T$ .

Additional in-depth information of the inherent energetic changes can be obtained from the adsorption thermodynamic parameters. Generally, negative  $\Delta G^0$  and  $\Delta H^0$  values indicate that the adsorption process is spontaneous and exothermic, respectively, while positive values indicate the opposite mechanism. Moreover, the  $\Delta H^0$  values are also used to distinguish whether the adsorption process can be classified as physisorption or chemisorption. Physisorption processes are dominant below  $20 \text{ kJ mol}^{-1}$ , physisorption-

chemisorption processes are dominant at  $20\text{--}80 \text{ kJ mol}^{-1}$ , and chemisorption processes are dominant at  $80\text{--}400 \text{ kJ mol}^{-1}$  (Andersson et al., 2011).

### 5.4. Other pathways that accompany adsorption

In addition to the general adsorption mechanism (physical adsorption, electrostatic interaction, and surface interaction between the heavy metal ions and surface functional groups), other removal pathways may also occur, depending on the nanomaterial properties and additional characteristics provided by functionalization (Fig. 3).

Oxidation and reduction play significant roles in the interactions between heavy metal ions and functionalized carbon-based nanomaterials with redox capacity, especially during the removal of Cr(VI) and As(III). The reaction mechanism for MWCNTs supported nZVI nanocomposites prepared to remove Cr(VI) included the reduction of Cr(VI) to Cr(III) by the oxidation of nZVI to iron ions, which would precipitate soluble Cr to form  $\text{Cr}_x\text{Fe}_{1-x}(\text{OH})_3$  complexes on the nanomaterial surfaces and enhance the adsorption process (Lv et al., 2011). Since As(III) adsorption is always weaker than that of As(V) by MWCNTs and other adsorbents, a pretreatment for oxidizing As(III) to As(V) is required to achieve satisfactory As(III) removal. The removal pathway of As(III) by GO-Mn<sub>2</sub>O<sub>3</sub> nanohybrids involved oxidation of As(III) to As(V) by the manganese oxide, which created more active sites for the adsorption process (Kumar et al., 2014).

Hydrolysis, flocculation, complexation, precipitation, and ion exchange also may contribute to the removal of heavy metal ions by functionalized carbon-based nanomaterials. For example, non-specific ion exchange between GO and Pb(II) was indicated by the binding energy peak at 137.8 eV in XPS spectra of Pb-laden GO, and inner-sphere complexation between HMO and Pb(II) was implied by the peak forwarded to 137.0 eV in the XPS spectra of Pb-laden HMO@GO (Wan et al., 2016). Cui et al. modified the surface of GO with CHAP, which had strong ion exchange properties and could enhance the Pb(II) removal (Cui et al., 2015).

## 6. Future research prospects

### 6.1. Functional nanomaterials for treating combined pollution

In most cases, water environmental chemistry is very complicated. The water contains many kinds of pollutants, which give rise to more serious environmental damage from their combined toxicities and relative mobility. Developing highly effective methods to

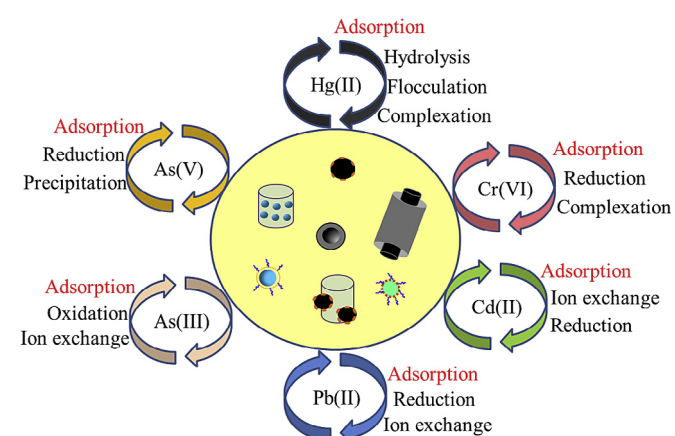


Fig. 3. Pathways for aqueous heavy metal removal by functionalized nanomaterials.

remove hazardous pollutants from water simultaneously has become a well-researched topic that addresses an urgent demand for practical applications in water pollution control (Luo et al., 2011; Tao et al., 2016; Yan et al., 2016).

Some active substances with good affinity toward a wide range of contaminants have been used to modify the NPs and enhance their pollutant removal efficiencies (Cai et al., 2010; Khan et al., 2015). Fig. 4 shows some examples that two or more contaminants were simultaneously removed from water by functionalized carbon nanomaterials, including GO-zirconium phosphate (GO-Zr-P) nanomaterials, titanium and lanthanum oxides impregnated on granular activated carbon (Ti/La-AC), and nitrogen-functionalized magnetic ordered mesoporous carbon (N-Fe/OMC) (Jing et al., 2012; Pourbeyram, 2016; Yang et al., 2015). Additionally, in our previous study, it has been proved that zero valent iron is a strong reducible agent that can remove not only heavy metal ions (Cr), but also  $\text{NO}_3^-$  and chlorinated organics (2,4-dichlorophenol) (Lv et al., 2012; Xu et al., 2012a, 2013a, 2016a). Iron-based functionalized nanomaterials are also expected to treat combined heavy metal and halogenated organic pollution.

Research on the removal of combined pollution by carbon-based nanomaterials is still lacking, and researchers need to consider potential coexisting pollutants when studying the removal of a given pollutant. It is important to synthesize more functional nanomaterials that can remove a wide range of contaminants, maintain good activity for a long time, and meet the requirements for the practical treatment of wastewater.

## 6.2. Sustainability of nanomaterials

Although novel and functionalized nanomaterials have good potential to improve the performance of current and future technologies in many fields, environmental implications (e.g., fate, transport, and ecotoxicity) should be concerned due to the discharge of engineered nanomaterials, in order to reduce (or even preclude) the potential of adverse unintended consequences. Since the application (e.g., adsorption capacity) and implication (e.g., toxicity) depend on physicochemical properties (e.g., size, functional groups, surface charge, purity and so on), sustainability by design is a framework that aims to synthesize engineered nanomaterials not only to be safe to the environment and humans, but also to meet the desired performance. The relationships between the structure design, obtained function, and environmental risk of engineered nanomaterials are desired to be studied and established.

Additionally, the production impacts of CNTs were reported to exceed their direct exposure impacts (Eckelman et al., 2012), and the lens of toxicity assessment of CNTs and graphene nanomaterials

need to be broadened, which requires to include the impacts of whole life cycle, rather than prioritizing direct exposure impacts. Both the environmental direct-release impacts and production-side impacts of CNT and graphene nanomaterials are required to be mitigated. Future development into improving the environmental sustainability of CNTs and graphene nanomaterials should take a life cycle perspective to balance the commercial-production economics, application performance, and environmental implication.

## 6.3. Computational simulations

Computational chemistry has been applied to simulate the heterogeneous reactions of heavy metals by nanomaterials functionalized with metals, metal oxides, or carbon (Siddiqui et al., 2013; Hou et al., 2014; Xu et al., 2015). Insight into the removal reactions at the molecular-electronic level can be gained by computational simulation via theoretical calculations, including *ab initio* methods, the density functional theory (DFT), and their derivative models (Steckel, 2008; Sun et al., 2011; Wilcox and Okano, 2011). Thermodynamic properties, accurate bond energies, some experimental kinetic parameters that are difficult to deduce, and a better description of the reaction mechanism can be obtained from the models (Auzmendi-Murua et al., 2014; Wang et al., 2015b). The results contribute to the design and modification of functional nanomaterials to improve their absorptive efficiencies for heavy metals. However, most of these studies were focused on the gas phase, especially for mercury oxidization and adsorption from flue gas.

Few studies have focused on the optimization of nanomaterial fabrication. Roohi and Khyrkhan investigated the structural and electronic properties of green chemically functionalized SWCNTs with IL functional groups via DFT, including the distances and strength of hydrogen bonds in the IL and the length of the  $\text{C}=\text{C}$  bonds in the SWCNTs (Roohi and Khyrkhan, 2015). It was suggested that IL preferred the edge site of pristine SWCNTs rather than other positions, based on the relative energies. However, further studies on computer simulations of the interaction between heavy metal ions and nanomaterials in aqueous phase are still needed to save valuable time and effort during basic lab experiments.

## 6.4. Other recommendations for future research

Although the development of functionalized nanomaterials has received much attention recently, there is still a long way to go before achieving the ultimate goal of practical application and commercialization.

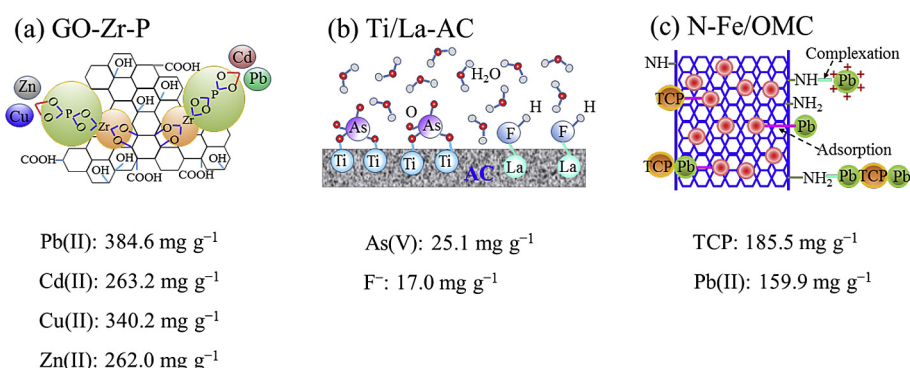


Fig. 4. Schematic of functionalized nanomaterials for combined pollutant removal.

- i. The properties of nanomaterials are mainly dependent on the preparation methods and conditions, which play an important role in the sizes, structures, compositions, and reaction activities of functionalized nanomaterials. Few studies have investigated the effects of preparation conditions on the functionalized nanomaterials, including reaction time, reagent, temperature, and pH. We should focus on these influencing factors not only during the removal reaction, but also in the preparation process.
- ii. Functionalized nanomaterials need to be applied to treat actual wastewater, rather than simulated water that only contains one heavy metal ion and few substances, in lab-scale batch experiments. More column and field studies are also needed.
- iii. Most studies have focused on the removal efficiencies and capacities of heavy metals. More attention needs to be paid to the costs of using and supporting facilities required for the use of functionalized nanomaterials. Recycling of the nanomaterials also needs to be further explored. The resulting waste products will likely require further treatment due to the hazardous nature of heavy metals and ecological risks of some nanomaterials.

## 7. Conclusions

This review highlighted carbon nanotubes-based and graphene-based nanomaterials used for the adsorption of selected aqueous heavy metal ions, especially the most common and toxic metals, including Hg(II), Pb(II), Cr(VI), Cd(II), and As(III)/(V). Bare, oxidized, and various modified carbon-based nanomaterials have been employed to adsorb aqueous heavy metals, and better adsorption performance and higher adsorptive capacity are achieved after functionalization. The preparations, characterizations, and applications of carbon-based nanomaterials used to adsorb aqueous heavy metals in recent years were summarized. The effects of temperature, pH, ionic strength, and coexisting ions on the adsorption of aqueous heavy metals by functionalized carbon-based nanomaterials were discussed, as well as the adsorption isotherms, kinetics, thermodynamics, and other relevant mechanisms. However, further research work is still needed to focus on the preparation of more refined carbon-based nanomaterials for wastewater with combined pollutants.

## Acknowledgements

This work was supported by the Chenguang Program of Shanghai Education Development Foundation and Shanghai Municipal Education Commission (No. 16CG23) and the National Key Research and Development Program of China (2016YFC0402600).

## References

- Addo Ntim, S., Mitra, S., 2012. Adsorption of arsenic on multiwall carbon nanotube–zirconia nanohybrid for potential drinking water purification. *J. Colloid Interface Sci.* 375, 154–159.
- Addo Ntim, S., Mitra, S., 2011. Removal of trace arsenic to meet drinking water standards using iron oxide coated multiwall carbon nanotubes. *J. Chem. Eng. Data* 56, 2077–2083.
- Akhavan, B., Jarvis, K., Majewski, P., 2015. Plasma polymer-functionalized silica particles for heavy metals removal. *ACS Appl. Mater. Interfaces* 7, 4265–4274.
- Aljani, H., Shariatinia, Z., 2017. Effective aqueous arsenic removal using zero valent iron doped MWCNT synthesized by *in situ* CVD method using natural  $\alpha$ -Fe<sub>2</sub>O<sub>3</sub> as a precursor. *Chemosphere* 171, 502–511.
- AlOmar, M.K., Alsaadi, M.A., Hayyan, M., Akib, S., Ibrahim, M., Hashim, M.A., 2017. Allyl triphenyl phosphonium bromide based DES-functionalized carbon nanotubes for the removal of mercury from water. *Chemosphere* 167, 44–52.
- Andersson, K.I., Eriksson, M., Norgren, M., 2011. Removal of lignin from wastewater generated by mechanical pulping using activated charcoal and fly ash: adsorption isotherms and thermodynamics. *Ind. Eng. Chem. Res.* 50, 7722–7732.
- Atieh, M.A., 2011. Removal of chromium (VI) from polluted water using carbon nanotubes supported with activated carbon. *Procedia Environ. Sci.* 4, 281–293.
- Auzmendi-Murua, I., Castillo, A., Bozzelli, J.W., 2014. Mercury oxidation via chlorine, bromine, and iodine under atmospheric conditions: thermochemistry and kinetics. *J. Phys. Chem. A* 118, 2959–2975.
- Bandaru, N.M., Reta, N., Dalal, H., Ellis, A.V., Shapter, J., Voelcker, N.H., 2013. Enhanced adsorption of mercury ions on thiol derivatized single wall carbon nanotubes. *J. Hazard. Mater.* 261, 534–541.
- Boenigk, D.W., 2000. Ecological effects, transport, and fate of mercury: a general review. *Chemosphere* 40, 1335–1351.
- Cai, G., Zhao, G., Wang, X., Yu, S., 2010. Synthesis of polyacrylic acid stabilized amorphous calcium carbonate nanoparticles and their application for removal of toxic heavy metal ions in water. *J. Phys. Chem. C* 114, 12948–12954.
- Chabot, V., Higgins, D., Yu, A., Xiao, X., Chen, Z., Zhang, J., 2014. A review of graphene and graphene oxide sponge: material synthesis and applications to energy and the environment. *Energy Environ. Sci.* 7, 1564–1596.
- Chandra, V., Park, J., Chun, Y., Lee, J.W., Hwang, I., Kim, K.S., 2010. Water-dispersible magnetite-reduced graphene oxide composites for arsenic removal. *ACS Nano* 4, 3979–3986.
- Chang, H., Wu, H., 2013. Graphene-based nanocomposites: preparation, functionalization, and energy and environmental applications. *Energy Environ. Sci.* 6, 3483–3507.
- Chen, B., Zhu, Z., Ma, J., Yang, M., Hong, J., Hu, X., Qiu, Y., Chen, J., 2014a. One-pot, solid-phase synthesis of magnetic multiwalled carbon nanotube/iron oxide composites and their application in arsenic removal. *J. Colloid Interface Sci.* 434, 9–17.
- Chen, P.H., Hsu, C., Tsai, D.D., Lu, Y., Huang, W., 2014b. Adsorption of mercury from water by modified multi-walled carbon nanotubes: adsorption behaviour and interference resistance by coexisting anions. *Environ. Technol.* 35, 1935–1944.
- Cho, H., Wepasnick, K., Smith, B.A., Bangash, F.K., Fairbrother, D.H., Ball, W.P., 2010. Sorption of aqueous Zn[II] and Cd[II] by multiwall carbon nanotubes: the relative roles of oxygen-containing functional groups and graphenic carbon. *Langmuir* 26, 967–981.
- Chowdhury, S.R., Yanful, E.K., Pratt, A.R., 2010. Arsenic removal from aqueous solutions by mixed magnetite–maghemite nanoparticles. *Environ. Earth Sci.* 64, 411–423.
- Cui, L., Wang, Y., Hu, L., Gao, L., Du, B., Wei, Q., 2015. Mechanism of Pb(II) and methylene blue adsorption onto magnetic carbonate hydroxyapatite/graphene oxide. *RSC Adv.* 5, 9759–9770.
- Cui, L., Yang, Y., Hsu, C., Cui, Y., 2009. Carbon–silicon core–shell nanowires as high capacity electrode for lithium ion batteries. *Nano Lett.* 9, 3370–3374.
- Cutting, R.S., Coker, V.S., Telling, N.D., Kimber, R.L., Pearce, C.I., Ellis, B.L., Lawson, R.S., van der Laan, G., Patrick, R.A.D., Vaughan, D.J., Arenholz, E., Lloyd, J.R., 2010. Optimizing Cr(VI) and Tc(VII) remediation through nanoscale biomimetic engineering. *Environ. Sci. Technol.* 44, 2577–2584.
- Di, Z., Ding, J., Peng, X., Li, Y., Luan, Z., Liang, J., 2006. Chromium adsorption by aligned carbon nanotubes supported ceria nanoparticles. *Chemosphere* 62, 861–865.
- Dichiara, A.B., Webber, M.R., Gorman, W.R., Rogers, R.E., 2015. Removal of copper ions from aqueous solutions via adsorption on carbon nanocomposites. *ACS Appl. Mater. Interfaces* 7, 15674–15680.
- Dong, H., Lin, Z., Wan, X., Feng, L., 2017. Risk assessment for the mercury polluted site near a pesticide plant in Changsha, Hunan, China. *Chemosphere* 169, 333–341.
- Du, Y., Liu, W., Qiang, R., Wang, Y., Han, X., Ma, J., Xu, P., 2014. Shell thickness-dependent microwave absorption of core–shell Fe<sub>3</sub>O<sub>4</sub>@C composites. *ACS Appl. Mater. Interfaces* 6, 12997–13006.
- Eckelman, M.J., Mauter, M.S., Isaacs, J.A., Elimelech, M., 2012. New perspectives on nanomaterial aquatic ecotoxicity: production impacts exceed direct exposure impacts for carbon nanotubes. *Environ. Sci. Technol.* 46, 2902–2910.
- El-Sheikh, A.H., Al-Degs, Y.S., Al-As'ad, R.M., Sweileh, J.A., 2011. Effect of oxidation and geometrical dimensions of carbon nanotubes on Hg(II) sorption and pre-concentration from real waters. *Desalination* 270, 214–220.
- Gardarin, A., Chédin, S., Lagniel, G., Aude, J., Godat, E., Catty, P., Labarre, J., 2010. Endoplasmic reticulum is a major target of cadmium toxicity in yeast. *Mol. Microbiol.* 76, 1034–1048.
- Ge, Y., Li, Z., Xiao, D., Xiong, P., Ye, N., 2014. Sulfonated multi-walled carbon nanotubes for the removal of copper (II) from aqueous solutions. *J. Ind. Eng. Chem.* 20, 1765–1771.
- George, R., Bahadur, N., Singh, N., Singh, R., Verma, A., Shukla, A.K., 2016. Environmentally benign TiO<sub>2</sub> nanomaterials for removal of heavy metal ions with interfering ions present in tap water. *Mater. Today Proceed.* 3, 162–166.
- Gollavelli, G., Chang, C., Ling, Y., 2013. Facile synthesis of smart magnetic graphene for safe drinking water: heavy metal removal and disinfection control. *ACS Sustain. Chem. Eng.* 1, 462–472.
- Gupta, A., Vidyarthi, S.R., Sankararamakrishnan, N., 2014. Enhanced sorption of mercury from compact fluorescent bulbs and contaminated water streams using functionalized multiwalled carbon nanotubes. *J. Hazard. Mater.* 274, 132–144.
- Gupta, V.K., Rastogi, A., 2008. Sorption and desorption studies of chromium(VI) from nonviable cyanobacterium *Nostoc muscorum* biomass. *J. Hazard. Mater.* 154, 347–354.

- Hadavifar, M., Bahramifar, N., Younesi, H., Li, Q., 2014. Adsorption of mercury ions from synthetic and real wastewater aqueous solution by functionalized multi-walled carbon nanotube with both amino and thiolated groups. *Chem. Eng. J.* 237, 217–228.
- Hahm, M.G., Lee, J., Hart, A.H.C., Song, S.M., Nam, J., Jung, H.Y., Hashim, D.P., Li, B., Narayanan, T.N., Park, C., Zhao, Y., Vajtai, R., Kim, Y.A., Hayashi, T., Ku, B., Endo, M., Barreira, E., Jung, Y.J., Thomas, E.L., Ajayan, P.M., 2013. Carbon nanotube core graphitic shell hybrid fibers. *ACS Nano* 7, 10971–10977.
- Han, W.S., Lee, H.Y., Jung, S.H., Lee, S.J., Jung, J.H., 2009. Silica-based chromogenic and fluorogenic hybrid chemosensor materials. *Chem. Soc. Rev.* 38, 1904–1915.
- Hashim, M.A., Mukhopadhyay, S., Sahu, J.N., Sengupta, B., 2011. Remediation technologies for heavy metal contaminated groundwater. *J. Environ. Manag.* 92, 2355–2388.
- Hou, W., Zhou, J., Yu, C., You, S., Gao, X., Luo, Z., 2014. Pd/Al2O3 sorbents for elemental mercury capture at high temperatures in syngas. *Ind. Eng. Chem. Res.* 53, 9909–9914.
- Huang, J., Yuan, F., Zeng, G., Li, X., Gu, Y., Shi, L., Liu, W., Shi, Y., 2017. Influence of pH on heavy metal speciation and removal from wastewater using micellar-enhanced ultrafiltration. *Chemosphere* 173, 199–206.
- Huang, Y., Wu, D., Wang, X., Huang, W., Lawless, D., Feng, X., 2016. Removal of heavy metals from water using polyvinylamine by polymer-enhanced ultrafiltration and flocculation. *Sep. Purif. Technol.* 158, 124–136.
- Hummers, W.S., Offeman, R.E., 1958. Preparation of graphitic oxide. *J. Am. Chem. Soc.* 80, 1339.
- Ihsanullah Abbas, A., Al-Amer, A.M., Laoui, T., Al-Marri, M.J., Nasser, M.S., Khrisheh, M., Atieh, M.A., 2016. Heavy metal removal from aqueous solution by advanced carbon nanotubes: critical review of adsorption applications. *Sep. Purif. Technol.* 157, 141–161.
- Jabeen, H., Kemp, K.C., Chandra, V., 2013. Synthesis of nano zerovalent iron nanoparticles – graphene composite for the treatment of lead contaminated water. *J. Environ. Manag.* 130, 429–435.
- Jastrzębska, A.M., Karcz, J., Letmanowski, R., Zabost, D., Ciecielska, E., Zdunek, J., Karwowska, E., Siekierski, M., Olszyna, A., Kunicki, A., 2016. Synthesis of the GO/Al2O3 core–shell nanocomposite flakes and characterization of their unique electrostatic properties using zeta potential measurements. *Appl. Surf. Sci.* 362, 577–594.
- Ji, L., Zhou, L., Bai, X., Shao, Y., Zhao, G., Qu, Y., Wang, C., Li, Y., 2012. Facile synthesis of multiwall carbon nanotubes/iron oxides for removal of tetrabromobisphenol A and Pb(ii). *J. Mater. Chem.* 22, 15853–15862.
- Jin, Z., Gao, H., Hu, L., 2015. Removal of Pb(ii) by nano-titanium oxide investigated by batch, XPS and model techniques. *RSC Adv.* 5, 88520–88528.
- Jing, C., Cui, J., Huang, Y., Li, A., 2012. Fabrication, characterization, and application of a composite adsorbent for simultaneous removal of arsenic and fluoride. *ACS Appl. Mater. Interfaces* 4, 714–720.
- Jung, Y., Kim, S., Park, S., Kim, J.M., 2008. Preparation of functionalized nanoporous carbons for uranium loading. *Colloid Surf. A* 313–314, 292–295.
- Khan, M.A., Ahmad, A., Umar, K., Nabi, S.A., 2015. Synthesis, characterization, and biological applications of nanocomposites for the removal of heavy metals and dyes. *Ind. Eng. Chem. Res.* 54, 76–82.
- Khin, M.M., Nair, A.S., Babu, V.J., Murugan, R., Ramakrishna, S., 2012. A review on nanomaterials for environmental remediation. *Energy Environ. Sci.* 5, 8075–8109.
- Krishna Kumar, A.S., Jiang, S., Tseng, W., 2015. Effective adsorption of chromium(vi)/Cr(iii) from aqueous solution using ionic liquid functionalized multiwalled carbon nanotubes as a super sorbent. *J. Mater. Chem. A* 3, 7044–7057.
- Kumar, R., Ansari, M.O., Barakat, M.A., 2013. DBSA doped polyaniline/multi-walled carbon nanotubes composite for high efficiency removal of Cr(VI) from aqueous solution. *Chem. Eng. J.* 228, 748–755.
- Kumar, S., Nair, R.R., Pillai, P.B., Gupta, S.N., Iyengar, M.A.R., Sood, A.K., 2014. Graphene oxide–MnFe2O4 magnetic nanohybrids for efficient removal of lead and arsenic from water. *ACS Appl. Mater. Interfaces* 6, 17426–17436.
- Kwon, O., Kim, J., Cho, D., Kumar, R., Baek, S.H., Kurade, M.B., Jeon, B., 2016. Adsorption of As(III), As(V) and Cu(II) on zirconium oxide immobilized alginate beads in aqueous phase. *Chemosphere* 160, 126–133.
- Lavoie, R.A., Kyser, T.K., Friesen, V.L., Campbell, L.M., 2015. Tracking overwintering areas of fish-eating birds to identify mercury exposure. *Environ. Sci. Technol.* 49, 863–872.
- Li, Y., Ding, J., Luan, Z., Di, Z., Zhu, Y., Xu, C., Wu, D., Wei, B., 2003. Competitive adsorption of Pb<sup>2+</sup>, Cu<sup>2+</sup> and Cd<sup>2+</sup> ions from aqueous solutions by multiwalled carbon nanotubes. *Carbon* 41, 2787–2792.
- Liang, J., Liu, J., Yuan, X., Dong, H., Zeng, G., Wu, H., Wang, H., Liu, J., Hua, S., Zhang, S., Yu, Z., He, X., He, Y., 2015. Facile synthesis of alumina-decorated multi-walled carbon nanotubes for simultaneous adsorption of cadmium ion and trichloroethylene. *Chem. Eng. J.* 273, 101–110.
- Lin, T., Wu, J., 2001. Adsorption of arsenite and arsenate within activated alumina grains: equilibrium and kinetics. *Water Res.* 35, 2049–2057.
- Liu, M., Wen, T., Wu, X., Chen, C., Hu, J., Li, J., Wang, X., 2013a. Synthesis of porous Fe<sub>3</sub>O<sub>4</sub> hollow microspheres/graphene oxide composite for Cr(vi) removal. *Dalton Trans.* 42, 14710–14717.
- Liu, X., Wang, M., Zhang, S., Pan, B., 2013b. Application potential of carbon nanotubes in water treatment: a review. *J. Environ. Sci.* 25, 1263–1280.
- Lu, C., Chiu, H., Liu, C., 2006. Removal of Zinc(II) from aqueous solution by purified carbon nanotubes: kinetics and equilibrium studies. *Ind. Eng. Chem. Res.* 45, 2850–2855.
- Luo, C., Liu, C., Wang, Y., Liu, X., Li, F., Zhang, G., Li, X., 2011. Heavy metal contamination in soils and vegetables near an e-waste processing site, south China. *J. Hazard. Mater.* 186, 481–490.
- Lv, X.S., Xu, J., Jiang, G.M., Xu, X.H., 2011. Removal of chromium(VI) from wastewater by nanoscale zero-valent iron particles supported on multiwalled carbon nanotubes. *Chemosphere* 85, 1204–1209.
- Lv, X.S., Xu, J., Jiang, G.M., Tang, J., Xu, X.H., 2012. Highly active nanoscale zero-valent iron (nZVI)-Fe<sub>3</sub>O<sub>4</sub> nanocomposites for the removal of chromium(VI) from aqueous solutions. *J. Colloid Interface Sci.* 369, 460–469.
- Ma, J., Yang, M., Yu, F., Chen, J., 2015. Easy solid-phase synthesis of pH-insensitive heterogeneous CNTs/FeS Fenton-like catalyst for the removal of antibiotics from aqueous solution. *J. Colloid Interface Sci.* 444, 24–32.
- Ma, S., Zhan, S., Jia, Y., Zhou, Q., 2015. Highly efficient antibacterial and Pb(II) removal effects of Ag-CoFe<sub>2</sub>O<sub>4</sub>-GO nanocomposite. *ACS Appl. Mater. Interfaces* 7, 10576–10586.
- Machell, J., Prior, K., Allan, R., Andresen, J.M., 2015. The water energy food nexus – challenges and emerging solutions. *Environ. Sci. Water Res. Technol.* 1, 15–16.
- Madadragi, C.J., Kim, H.Y., Gao, G., Wang, N., Zhu, J., Feng, H., Gorring, M., Kasner, M.L., Hou, S., 2012. Adsorption behavior of EDTA-graphene oxide for Pb (II) removal. *ACS Appl. Mater. Interfaces* 4, 1186–1193.
- Mauter, M.S., Elimelech, M., 2008. Environmental applications of carbon-based nanomaterials. *Environ. Sci. Technol.* 42, 5843–5859.
- Meng, B., Feng, X., Qiu, G., Anderson, C.W.N., Wang, J., Zhao, L., 2014. Localization and speciation of mercury in brown rice with implications for pan-Asian public health. *Environ. Sci. Technol.* 48, 7974–7981.
- Mishra, A.K., Ramaprabhu, S., 2010. Magnetite decorated multiwalled carbon nanotube based supercapacitor for arsenic removal and desalination of seawater. *J. Phys. Chem. C* 114, 2583–2590.
- Mishra, A.K., Ramaprabhu, S., 2011. Functionalized graphene sheets for arsenic removal and desalination of sea water. *Desalination* 282, 39–45.
- Mobasherpoor, I., Salahi, E., Ebrahimi, M., 2012. Removal of divalent nickel cations from aqueous solution by multi-walled carbon nano tubes: equilibrium and kinetic processes. *Res. Chem. Intermed.* 38, 2205–2222.
- Moghaddam, H.K., Pakizeh, M., 2015. Experimental study on mercury ions removal from aqueous solution by MnO<sub>2</sub>/CNTs nanocomposite adsorbent. *J. Ind. Eng. Chem.* 21, 221–229.
- Moradi, O., 2011. The removal of ions by functionalized carbon nanotube: equilibrium, isotherms and thermodynamic studies. *Chem. Biochem. Eng. Q.* 229–240.
- Morillo, D., Pérez, G., Valiente, M., 2015. Efficient arsenic(V) and arsenic(III) removal from acidic solutions with novel forager sponge-loaded superparamagnetic iron oxide nanoparticles. *J. Colloid Interface Sci.* 453, 132–141.
- Mubarak, N.M., Alicia, R.F., Abdullah, E.C., Sahu, J.N., Haslila, A.B.A., Tan, J., 2013. Statistical optimization and kinetic studies on removal of Zn<sup>2+</sup> using functionalized carbon nanotubes and magnetic biochar. *J. Environ. Chem. Eng.* 1, 486–495.
- Ojani, R., Akbar, Z., Hasheminejad, E., Raof, J., 2014. Rapid fabrication of Cu/Pd nano/micro-particles porous-structured catalyst using hydrogen bubbles dynamic template and their enhanced catalytic performance for formic acid electrooxidation. *Int. J. Hydrogen Energy* 39, 7788–7797.
- Parambath, V.B., Nagar, R., Sethupathi, K., Ramaprabhu, S., 2011. Investigation of spillover mechanism in palladium decorated hydrogen exfoliated functionalized graphene. *J. Phys. Chem. C* 115, 15679–15685.
- Paul, B., Parashar, V., Mishra, A., 2015. Graphene in the Fe<sub>3</sub>O<sub>4</sub> nano-composite switching the negative influence of humic acid coating into an enhancing effect in the removal of arsenic from water. *Environ. Sci. Water Res. Technol.* 1, 77–83.
- Pendergast, M.M., Hoek, E.M.V., 2011. A review of water treatment membrane nanotechnologies. *Energy Environ. Sci.* 4, 1946–1971.
- Perreault, F., Fonseca de Faria, A., Elimelech, M., 2015. Environmental applications of graphene-based nanomaterials. *Chem. Soc. Rev.* 44, 5861–5896.
- Pillary, K., Cukrowska, E.M., Coville, N.J., 2009. Multi-walled carbon nanotubes as adsorbents for the removal of parts per billion levels of hexavalent chromium from aqueous solution. *J. Hazard. Mater.* 166, 1067–1075.
- Pourbeyram, S., 2016. Effective removal of heavy metals from aqueous solutions by graphene oxide–zirconium phosphate (GO–Zr-P) nanocomposite. *Ind. Eng. Chem. Res.* 55, 5608–5617.
- Qiu, B., Gu, H., Yan, X., Guo, J., Wang, Y., Sun, D., Wang, Q., Khan, M., Zhang, X., Weeks, B.L., Young, D.P., Guo, Z., Wei, S., 2014. Cellulose derived magnetic mesoporous carbon nanocomposites with enhanced hexavalent chromium removal. *J. Mater. Chem. A* 2, 17454–17462.
- Ray, P.Z., Shipley, H.J., 2015. Inorganic nano-adsorbents for the removal of heavy metals and arsenic: a review. *RSC Adv.* 5, 29885–29907.
- Rehman, Z.U., Khan, S., Brusseau, M.L., Shah, M.T., 2017. Lead and cadmium contamination and exposure risk assessment via consumption of vegetables grown in agricultural soils of five-selected regions of Pakistan. *Chemosphere* 168, 1589–1596.
- Ren, X., Shao, D., Zhao, G., Sheng, G., Hu, J., Yang, S., Wang, X., 2011. Plasma induced multiwalled carbon nanotube grafted with 2-vinylpyridine for preconcentration of Pb(II) from aqueous solutions. *Plasma Process Polym.* 8, 589–598.
- Roohi, H., Khaykhah, S., 2015. Green chemical functionalization of single-wall carbon nanotube with methylimidazolium dicyanamid ionic liquid: a first principle computational exploration. *J. Mol. Liq.* 211, 498–505.
- Rosenzweig, S., Sorial, G.A., Sahle-Demessie, E., Mack, J., 2013. Effect of acid and alcohol network forces within functionalized multiwall carbon nanotubes bundles on adsorption of copper (II) species. *Chemosphere* 90, 395–402.
- Sandoval, R., Cooper, A.M., Aymar, K., Jain, A., Hristovski, K., 2011. Removal of arsenic

- and methylene blue from water by granular activated carbon media impregnated with zirconium dioxide nanoparticles. *J. Hazard. Mater.* 193, 296–303.
- Sankaram Krishnan, N., Jaiswal, M., Verma, N., 2014. Composite nanofloral clusters of carbon nanotubes and activated alumina: an efficient sorbent for heavy metal removal. *Chem. Eng. J.* 235, 1–9.
- Shao, L., Wang, X., Ren, Y., Wang, S., Zhong, J., Chu, M., Tang, H., Luo, L., Xie, D., 2016. Facile fabrication of magnetic cucurbit[6]uril/graphene oxide composite and application for uranium removal. *Chem. Eng. J.* 286, 311–319.
- Shawky, H.A., El-Assar, A.H.M., Abo-Zeid, D.E., 2012. Chitosan/carbon nanotube composite beads: preparation, characterization, and cost evaluation for mercury removal from wastewater of some industrial cities in Egypt. *J. Appl. Polym. Sci.* 125, E93–E101.
- Shih, M., 2005. An overview of arsenic removal by pressure-driven membrane processes. *Desalination* 172, 85–97.
- Shih, Y., Ke, C., Yu, C., Lu, C., Tseng, W., 2014. Combined tween 20-stabilized gold nanoparticles and reduced graphite oxide– $\text{Fe}_3\text{O}_4$  nanoparticle composites for rapid and efficient removal of mercury species from a complex matrix. *ACS Appl. Mater. Interfaces* 6, 17437–17445.
- Siddiqui, S.A., Bouarissa, N., Rasheed, T., Al-Assiri, M.S., 2013. Quantum chemical study of the interaction of elemental Hg with small neutral, anionic and cationic  $\text{Au}$  ( $n = 1–6$ ) clusters. *Mater. Res. Bull.* 48, 995–1002.
- Sima, J., Cao, X., Zhao, L., Luo, Q., 2015. Toxicity characteristic leaching procedure over- or under-estimates leachability of lead in phosphate-amended contaminated soils. *Chemosphere* 138, 744–750.
- Sounthararajah, D.P., Loganathan, P., Kandasamy, J., Vigneswaran, S., 2017. Removing heavy metals using permeable pavement system with a titanate nano-fibrous adsorbent column as a post treatment. *Chemosphere* 168, 467–473.
- Steckel, J.A., 2008. Density functional theory study of mercury adsorption on metal surfaces. *Phys. Rev. B* 77, 115412.
- Sun, J., Xu, Q., 2014. Functional materials derived from open framework templates/precursors: synthesis and applications. *Energy Environ. Sci.* 7, 2071–2100.
- Sun, L., Zhang, A., Su, S., Wang, H., Liu, J., Xiang, J., 2011. A DFT study of the interaction of elemental mercury with small neutral and charged silver clusters. *Chem. Phys. Lett.* 517, 227–233.
- Sun, Y., Lei, C., Khan, E., Chen, S.S., Tsang, D.C.W., Ok, Y.S., Lin, D., Feng, Y., Li, X., 2017. Nanoscale zero-valent iron for metal/metalloid removal from model hydraulic fracturing wastewater. *Chemosphere* 176, 315–323.
- Tang, J., Huang, Y., Gong, Y., Lyu, H., Wang, Q., Ma, J., 2016. Preparation of a novel graphene oxide/Fe-Mn composite and its application for aqueous Hg(II) removal. *J. Hazard. Mater.* 316, 151–158.
- Tang, W., Zeng, G., Gong, J., Liu, Y., Wang, X., Liu, Y., Liu, Z., Chen, L., Zhang, X., Tu, D., 2012. Simultaneous adsorption of atrazine and Cu(II) from wastewater by magnetic multi-walled carbon nanotube. *Chem. Eng. J.* 211–212, 470–478.
- Tao, X., Li, K., Yan, H., Yang, H., Li, A., 2016. Simultaneous removal of acid green 25 and mercury ions from aqueous solutions using glutamine modified chitosan magnetic composite microspheres. *Environ. Pollut.* 209, 21–29.
- Tawabini, B.S., Al-Khalidi, S.F., Khaled, M.M., Atieh, M.A., 2011. Removal of arsenic from water by iron oxide nanoparticles impregnated on carbon nanotubes. *J. Environ. Sci. Health A* 46, 215–223.
- Thakur, S., Das, G., Raul, P.K., Karak, N., 2013. Green one-step approach to prepare sulfur/reduced graphene oxide nanohybrid for effective mercury ions removal. *J. Phys. Chem. C* 117, 7636–7642.
- Tian, Y., Gao, B., Morales, V.L., Wu, L., Wang, Y., Muñoz-Carpena, R., Cao, C., Huang, Q., Yang, L., 2012. Methods of using carbon nanotubes as filter media to remove aqueous heavy metals. *Chem. Eng. J.* 210, 557–563.
- Tofighi, M.A., Mohammadi, T., 2011. Adsorption of divalent heavy metal ions from water using carbon nanotube sheets. *J. Hazard. Mater.* 185, 140–147.
- Velicković, Z., Vuković, G.D., Marinković, A.D., Moldovan, M., Perić-Grujić, A.A., Uskoković, P.S., Ristić, M., 2012. Adsorption of arsenate on iron(III) oxide coated ethylenediamine functionalized multiwall carbon nanotubes. *Chem. Eng. J.* 181–182, 174–181.
- Vuković, G.D., Marinković, A.D., Čolić, M., Ristić, M., Aleksić, R., Perić-Grujić, A.A., Uskoković, P.S., 2010. Removal of cadmium from aqueous solutions by oxidized and ethylenediamine-functionalized multi-walled carbon nanotubes. *Chem. Eng. J.* 157, 238–248.
- Vuković, G.D., Marinković, A.D., Škapin, S.D., Ristić, M., Aleksić, R., Perić-Grujić, A.A., Uskoković, P.S., 2011. Removal of lead from water by amino modified multi-walled carbon nanotubes. *Chem. Eng. J.* 173, 855–865.
- Vunain, E., Mishra, A.K., Mamba, B.B., 2016. Dendrimers, mesoporous silicas and chitosan-based nanosorbents for the removal of heavy-metal ions: a review. *Int. J. Biol. Macromol.* 86, 570–586.
- Wan, S., He, F., Wu, J., Wan, W., Gu, Y., Gao, B., 2016. Rapid and highly selective removal of lead from water using graphene oxide-hydrated manganese oxide nanocomposites. *J. Hazard. Mater.* 314, 32–40.
- Wang, C., Tao, S., Wei, W., Meng, C., Liu, F., Han, M., 2010. Multifunctional mesoporous material for detection, adsorption and removal of  $\text{Hg}^{2+}$  in aqueous solution. *J. Mater. Chem.* 20, 4635–4641.
- Wang, H., Yuan, X., Wu, Y., Chen, X., Leng, L., Wang, H., Li, H., Zeng, G., 2015a. Facile synthesis of polypyrrole decorated reduced graphene oxide– $\text{Fe}_3\text{O}_4$  magnetic composites and its application for the Cr(VI) removal. *Chem. Eng. J.* 262, 597–606.
- Wang, J., Yu, H., Geng, L., Liu, J., Han, L., Chang, L., Feng, G., Ling, L., 2015b. DFT study of Hg adsorption on M-substituted Pd(111) and PdM/ $\gamma$ -Al<sub>2</sub>O<sub>3</sub>(110) (M = Au, Ag, Cu) surfaces. *Appl. Surf. Sci.* 355, 902–911.
- Wang, H.J., Zhou, A.L., Peng, F., Yu, H., Chen, L.F., 2007a. Adsorption characteristic of acidified carbon nanotubes for heavy metal Pb(II) in aqueous solution. *Mater. Sci. Eng.* 466, 201–206.
- Wang, S., Gong, W., Liu, X., Yao, Y., Gao, B., Yue, Q., 2007b. Removal of lead(II) from aqueous solution by adsorption onto manganese oxide-coated carbon nanotubes. *Sep. Purif. Technol.* 58, 17–23.
- Wang, Q., Li, J., Chen, C., Ren, X., Hu, J., Wang, X., 2011. Removal of cobalt from aqueous solution by magnetic multiwalled carbon nanotube/iron oxide composites. *Chem. Eng. J.* 174, 126–133.
- Wang, Z., Xu, J., Hu, Y., Zhao, H., Zhou, J., Liu, Y., Lou, Z., Xu, X., 2016. Functional nanomaterials: study on aqueous Hg(II) adsorption by magnetic Fe3O4@SiO<sub>2</sub>-SH nanoparticles. *J. Taiwan Inst. Chem. E* 60, 394–402.
- Wen, T., Wu, X., Tan, X., Wang, X., Xu, A., 2013. One-pot synthesis of water-swellable Mg-Al layered double hydroxides and graphene oxide nanocomposites for efficient removal of As(V) from aqueous solutions. *ACS Appl. Mater. Interfaces* 5, 3304–3311.
- Wilcox, J., Okano, T., 2011. Ab initio-based mercury oxidation kinetics via bromine at postcombustion flue gas conditions. *Energy Fuel.* 25, 1348–1356.
- Xiao, K., Xu, F., Jiang, L., Dan, Z., Duan, N., 2016. The oxidative degradation of polystyrene resins on the removal of Cr(VI) from wastewater by anion exchange. *Chemosphere* 156, 326–333.
- Xu, H., Xie, J., Ma, Y., Qu, Z., Zhao, S., Chen, W., Huang, W., Yan, N., 2015. The cooperation of FeS<sub>n</sub> in a MnO<sub>x</sub> complex sorbent used for capturing elemental mercury. *Fuel* 140, 803–809.
- Xu, J., Cao, Z., Liu, X., Zhao, H., Xiao, X., Wu, J., Xu, X., Zhou, J.L., 2016a. Preparation of functionalized Pd/Fe<sub>3</sub>O<sub>4</sub>@MWCNTs nanomaterials for aqueous 2,4-dichlorophenol removal: interactions, influence factors, and kinetics. *J. Hazard. Mater.* 317, 656–666.
- Xu, J., Liu, X., Lowry, G.V., Cao, Z., Zhao, H., Zhou, J.L., Xu, X., 2016b. Dechlorination mechanism of 2,4-dichlorophenol by magnetic MWCNTs supported Pd/Fe nanohybrids: rapid adsorption, gradual dechlorination, and desorption of phenol. *ACS Appl. Mater. Interfaces* 8, 7333–7342.
- Xu, X., Schierz, A., Xu, N., Cao, X., 2016c. Comparison of the characteristics and mechanisms of Hg(II) sorption by biochars and activated carbon. *J. Colloid Interface Sci.* 463, 55–60.
- Xu, J., Hao, Z., Xie, C., Lv, X., Yang, Y., Xu, X., 2012a. Promotion effect of  $\text{Fe}^{2+}$  and Fe3O4 on nitrate reduction using zero-valent iron. *Desalination* 284, 9–13.
- Xu, J., Lv, X., Li, J., Li, Y., Shen, L., Zhou, H., Xu, X., 2012b. Simultaneous adsorption and dechlorination of 2,4-dichlorophenol by Pd/Fe nanoparticles with multi-walled carbon nanotube support. *J. Hazard. Mater.* 225–226, 36–45.
- Xu, J., Sheng, T., Hu, Y., Baig, S.A., Lv, X., Xu, X., 2013a. Adsorption-dechlorination of 2,4-dichlorophenol using two specified MWCNTs-stabilized Pd/Fe nanocomposites. *Chem. Eng. J.* 219, 162–173.
- Xu, J., Tan, L., Baig, S.A., Wu, D., Lv, X., Xu, X., 2013b. Dechlorination of 2,4-dichlorophenol by nanoscale magnetic Pd/Fe particles: effects of pH, temperature, common dissolved ions and humic acid. *Chem. Eng. J.* 231, 26–35.
- Xu, X., Cao, X., Zhao, L., 2013c. Comparison of rice husk- and dairy manure-derived biochars for simultaneously removing heavy metals from aqueous solutions: role of mineral components in biochars. *Chemosphere* 92, 955–961.
- Xu, L., Wang, T., Wang, J., Lu, A., 2017a. Occurrence, speciation and transportation of heavy metals in 9 coastal rivers from watershed of Laizhou Bay, China. *Chemosphere* 173, 61–68.
- Xu, Y., Zhang, C., Zhao, M., Rong, H., Zhang, K., Chen, Q., 2017b. Comparison of bioleaching and electrokinetic remediation processes for removal of heavy metals from wastewater treatment sludge. *Chemosphere* 168, 1152–1157.
- Xu, Y., Bai, H., Lu, G., Li, C., Shi, G., 2008. Flexible graphene films via the filtration of water-soluble noncovalent functionalized graphene sheets. *J. Am. Chem. Soc.* 130, 5856–5857.
- Yan, L., Wang, W., Li, X., Duan, J., Jing, C., 2016. Evaluating adsorption media for simultaneous removal of arsenate and cadmium from metallurgical wastewater. *J. Environ. Chem. Eng.* 4, 2795–2801.
- Yang, G., Tang, L., Zeng, G., Cai, Y., Tang, J., Pang, Y., Zhou, Y., Liu, Y., Wang, J., Zhang, S., Xiong, W., 2015. Simultaneous removal of lead and phenol contamination from water by nitrogen-functionalized magnetic ordered mesoporous carbon. *Chem. Eng. J.* 259, 854–864.
- Yang, S., Li, J., Shao, D., Hu, J., Wang, X., 2009. Adsorption of Ni(II) on oxidized multi-walled carbon nanotubes: effect of contact time, pH, foreign ions and PAA. *J. Hazard. Mater.* 166, 109–116.
- Yao, Y., Ma, C., Wang, J., Qiao, W., Ling, L., Long, D., 2015. Rational design of high-surface-area carbon nanotube/microporous carbon core-shell nanocomposites for supercapacitor electrodes. *ACS Appl. Mater. Interfaces* 7, 4817–4825.
- Yurekli, Y., 2016. Removal of heavy metals in wastewater by using zeolite nanoparticles impregnated polysulfone membranes. *J. Hazard. Mater.* 309, 53–64.
- Zhang, C., Sui, J., Li, J., Tang, Y., Cai, W., 2012. Efficient removal of heavy metal ions by thiol-functionalized superparamagnetic carbon nanotubes. *Chem. Eng. J.* 210, 45–52.
- Zhang, K., Dwivedi, V., Chi, C., Wu, J., 2010. Graphene oxide/ferric hydroxide composites for efficient arsenate removal from drinking water. *J. Hazard. Mater.* 182, 162–168.
- Zhao, G., Li, J., Ren, X., Chen, C., Wang, X., 2011a. Few-layered graphene oxide nanosheets as superior sorbents for heavy metal ion pollution management. *Environ. Sci. Technol.* 45, 10454–10462.
- Zhao, X., Lv, L., Pan, B., Zhang, W., Zhang, S., Zhang, Q., 2011b. Polymer-supported nanocomposites for environmental application: a review. *Chem. Eng. J.* 170, 381–394.
- Zhao, H., Liu, X., Cao, Z., Zhan, Y., Shi, X., Yang, Y., Zhou, J., Xu, J., 2016. Adsorption

- behavior and mechanism of chloramphenicols, sulfonamides, and non-antibiotic pharmaceuticals on multi-walled carbon nanotubes. *J. Hazard. Mater.* 310, 235–245.
- Zhao, X., Jia, Q., Song, N., Zhou, W., Li, Y., 2010. Adsorption of Pb(II) from an aqueous solution by titanium dioxide/carbon nanotube nanocomposites: kinetics, thermodynamics, and isotherms. *J. Chem. Eng. Data* 55, 4428–4433.
- Zhao, Y., Li, J., Zhang, S., Chen, H., Shao, D., 2013. Efficient enrichment of uranium(vi) on amidoximated magnetite/graphene oxide composites. *RSC Adv.* 3, 18952–18959.
- Zhu, J., Wei, S., Gu, H., Rapole, S.B., Wang, Q., Luo, Z., Haldolaarachchige, N., Young, D.P., Guo, Z., 2012. One-pot synthesis of magnetic graphene nanocomposites decorated with core@double-shell nanoparticles for fast chromium removal. *Environ. Sci. Technol.* 46, 977–985.
- Zong, P., Wang, S., Zhao, Y., Wang, H., Pan, H., He, C., 2013. Synthesis and application of magnetic graphene/iron oxides composite for the removal of U(VI) from aqueous solutions. *Chem. Eng. J.* 220, 45–52.